

Improved Recursive Electromechanical Oscillations Monitoring Scheme: A Novel Distributed Approach

Haris M. Khalid, *Member, IEEE* and Jimmy C.-H. Peng, *Member, IEEE*

Abstract—This paper improves the existing Kalman-based technique for detecting electromechanical oscillations using Synchrophasor measurements. The novelty is the utilization of a distributed architecture to extract maximum *a-posteriori* (MAP) estimations of oscillatory parameters. This was achieved by an expectation maximization (EM) algorithm. To improve initial condition estimation, initial correlation information through a forward backward (FB) Kalman-like particle filter (KLPF) was integrated into the proposed scheme. Performance evaluation was conducted using IEEE New England 39 Bus system and Synchrophasor measurements collected from New Zealand Grid. The proposed method accurately extracted oscillatory parameters when the measurements were contaminated by continuous random small load fluctuations. The method also improved the capability of detecting multiple oscillations with similar frequencies.

Index Terms—Distributed estimation, electromechanical oscillations, expectation maximization, forward-backward Kalman-like particle filter, inter-area oscillation, maximum *a-posteriori*, power system stability, Synchrophasor.

I. INTRODUCTION

ELECTROMECHANICAL oscillations are power transfers between groups of interconnected synchronous generators within the transmission system. Conservative power transfer limits are set to prevent lightly damped inter-area oscillations, which then lead to transmission bottlenecks [1, 2]. To increase transmission margins, Wide-Area Monitoring System (WAMS) was established [3]. WAMS allows real-time oscillatory parameters to be extracted using Synchrophasor measurements collected from Phasor Measurement Units (PMUs) installed at substations.

Oscillatory parameters are traditionally extracted using modal analysis [4–6]. Since linear state-space models cannot guarantee accurate representation of non-linear system dynamic characteristics, time-domain based techniques were introduced. These methods are primarily based on analyzing Synchrophasor measurements obtained from one location [7–14]. However, the short-coming of computing modal parameters from one location is that estimation errors may incur due to lack of observability. Another challenge among published methods are tracking oscillations having similar frequencies [15].

The contribution of this paper is to enhance the observability of inter-area oscillation, and improve the detection capability of electromechanical oscillations having similar frequencies. This is accomplished by revamping the oscillation state estimation, thus extracting MAP information using a proposed distributed detection scheme named as EM-based FB KLPF. The Kalman like Particle filter is preferred over the basic Kalman filter because it affords a better defined observation matrix [17]. The proposed scheme is based on extensions of the authors’

earlier works from [2] and [16]. This is attained by utilizing a distributed architecture and fusing system dynamics contained within multiple substation signals. An overview of the EM-based FB KLPF is illustrated in Fig.1. Compared with its Kalman predecessors of [2, 8], the proposed scheme is implied to improve the estimation accuracy under continuous random small load fluctuations. This is done by computing modal parameters at each PMU location. The proposed method is developed by considering an observation model for the state variables (See Fig. 1), followed by transformation of electromechanical oscillations into the frequency domain. MAP estimations are then calculated using EM-based FB KLPF. Next, the distributed filtering fusion is formulated. The processed parameters are sent into a master filter, which compute the error covariance matrix, $P_{t|t}$, and state estimate, $\hat{\alpha}_{t|t}$, of each state. Subsequently, the updated covariance matrix and state estimate values of the master filter are fed back to all metering locations. The proposed scheme provides a novel and convenient way to enhance the modal estimations at locations that are dominated by noise and system perturbations. It shall be noted that the oscillatory frequencies and corresponding damping factors are computed using the state representation of [2].

The paper is organized as follows: The proposed oscillation detection scheme is formulated in Section II. In Section III the implementation and evaluation on two test-cases are discussed, and finally conclusions are drawn in Section IV.

Notations: In this paper, a hat over a variable indicates an estimate of the variable e.g. $\hat{\alpha}$ is an estimate of α . The individual entries of a variable like α are denoted by $\alpha(l)$. When any of these variables becomes a function of time, the time index t appears as a subscript (e.g. we write $\alpha_t, C_t, \Upsilon_t$). The notation α_0^T is used to denote the sequence $(\alpha_0, \alpha_1, \dots, \alpha_T)$.

II. THE PROPOSED OSCILLATION DETECTION SCHEME

A. State Formulation with Observation Model

Consider a distributed discrete-time dynamical system as:

$$\alpha_{t+1} = \phi\alpha_t + v_t, \quad t = 0, 1, \dots, T \quad (1)$$

where $\alpha_0 \in \mathbf{R}^r$ is the initial condition of the oscillation state, $\phi \in \mathbf{R}^{r \times r}$ is a modal matrix of the oscillation response, such that it depends on covariates, $v_t \in \mathbf{R}^r$ is the random small load fluctuations based zero-mean white Gaussian noise, such that $\mathbf{E}[v_t] = 0$, t is the time instant and T is the number of time instants. Let the system described in (1) be monitored by a network of N sensors. It should be noted that the sensors are PMUs installed in high-voltage substations. Observations at i -th sensor with time instant t can be stated as:

$$\Upsilon_t^i = C_t^i \alpha_t + w_t^i, \quad i = 1, \dots, N \quad (2)$$

where $\Upsilon_t^i \in \mathbf{R}^{p^i}$ is the local observation output of oscillations at i -th sensor, p^i is the number of local simultaneous observa-

This work was funded by the Cooperative Agreement between the Masdar Institute of Science and Technology, Abu Dhabi, UAE and the Massachusetts Institute of Technology, Cambridge, MA.

The authors are with Department of Electrical Engineering and Computer Science, Institute Center for Energy, Masdar Institute of Science and Technology (MIST), Abu Dhabi, UAE. E-mail: mkhalid, jpeng@masdar.ac.ae

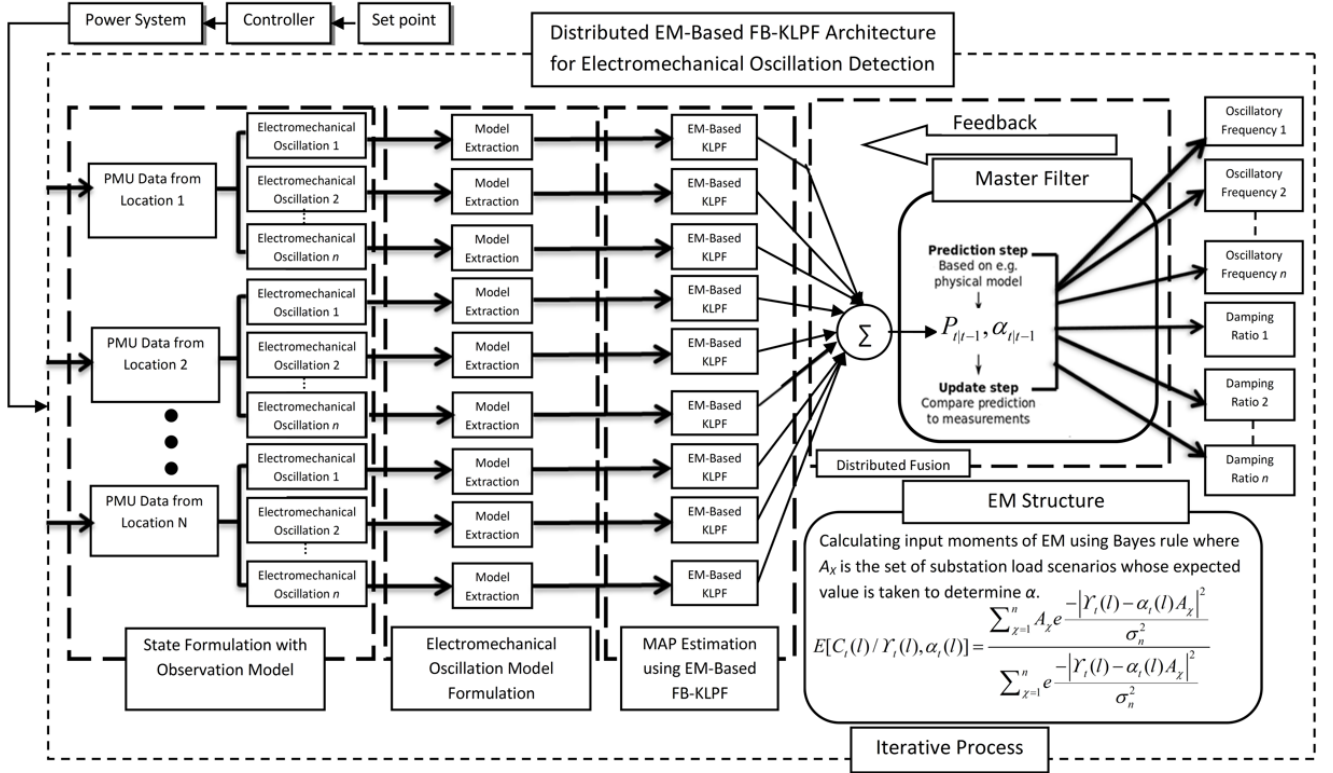


Fig. 1. Proposed Distributed Estimation Scheme for Monitoring Multiple Electromechanical Oscillations

tions for oscillations made by i -th sensor at time instant t , $C_t^i \in \mathbf{R}^{p^i \times r}$ is the local observation matrix for i -th sensor, α_t is the oscillation state matrix and $w_t^i \in \mathbf{R}^{p^i}$ is the local observation with zero-mean white Gaussian noise, such that $\mathbf{E}[w_t^i] = 0$, $\mathbf{E}[w_t^i w_t^{i*}] = R^i \delta_t^i$, where R^i represents the local covariance matrix and δ_t^i is a Kronecker delta function used for shifting integer variable for the presence or absence of noise accordingly. $\mathbf{E}[w_t^i w_t^{j*}] = 0$, and $\mathbf{E}[w_t^i w_t^{i*}] = Q \delta_t^i$, where Q is the process noise correlation factor. Observations from all N sensors in the network are integrated synthetically to the master oscillations observation output model $\Upsilon_{\text{master},t} \in \mathbf{R}^{p_{\text{master}}}$, subscript master, t represents the global observations gathered from the local i -th sensors at time instant t , p_{master} is the master oscillations observation output collected from number of local i -th sensors. Suppose the master observation matrix, $C_{\text{master},t} \in \mathbf{R}^{p_{\text{master}} \times r}$ and the master observation noise vector, $w_{\text{master},t} \in \mathbf{R}^{p_{\text{master}}}$ be:

$$\Upsilon_{\text{master},t} = \begin{bmatrix} \Upsilon_t^1 \\ \vdots \\ \Upsilon_t^N \end{bmatrix}, C_{\text{master},t} = \begin{bmatrix} C_t^1 \\ \vdots \\ C_t^N \end{bmatrix}, w_{\text{master},t} = \begin{bmatrix} w_t^1 \\ \vdots \\ w_t^N \end{bmatrix} \quad (3)$$

where N is the number of sensors. Then the master observation model at time t is given by:

$$\Upsilon_{\text{master},t} = C_{\text{master},t} \alpha_t + w_{\text{master},t}, \quad (4)$$

where $\Upsilon_{\text{master},t}$ is the master oscillations observation output vector, $C_{\text{master},t}$ is the master observation matrix, α_t is the oscillation state matrix, and $w_{\text{master},t}$ is the master observation noise vector. From equation (1) and (2), it is assumed that the pair $(\phi, C_{\text{master},t})$ is observable.

Once the observation model is extracted, the state represen-

tation of the oscillatory frequencies is followed.

B. Electromechanical Oscillation Model Formulation

As documented in [2], electromechanical oscillations can be represented as a sum of K exponentially damped sinusoidal waveforms with additive observation noise w_t . Therefore, considering the domain transformation for frequency oscillations, the local observation oscillation output signal Υ_t^i from an i -th sensor at time t is modeled as:

$$\Upsilon_t^i = \sum_{k=1}^K b_k e^{\lambda_k t T_s} + w_t^i, \text{ for } t = 1, 2, \dots, T \quad (5)$$

where a_k represents the complex amplitude of the k -th mode, λ_k is the k -th eigenvalue of that particular oscillatory mode and T_s is the sampling interval. By decomposing λ_k into its rectangular complex form, the signal becomes:

$$\Upsilon_t^i = \sum_{k=1}^K a_k e^{(-\sigma_k + j2\pi f_k)t T_s} + w_t^i, \text{ for } t = 1, 2, \dots, T \quad (6)$$

where σ_k and f_k are the damping factor and the oscillatory frequency extracted from the oscillation at i -th substation, respectively. Referring to [2], the k -th eigenvalue of a particular oscillatory mode is represented by two oscillation states denoted as $\alpha_{t,k}$ and $\alpha_{t,k+1}$, respectively. They can be expressed as:

$$\alpha_{t,k}^i = e^{(-\sigma_k + j2\pi f_k)t T_s}, \alpha_{t,k+1}^i = a_k e^{(-\sigma_k + j2\pi f_k)t T_s} \quad (7)$$

Thus, a signal consisting of K number of exponentially damped sinusoids is modeled by $2K$ number of oscillation states.

To find the damping factor σ_k and oscillatory frequency f_k , the computation of individual oscillation state α_t is required. The direct computation of α_t is not reasonable because C_t is

an unobserved oscillation latent variable. Therefore, a regularization method is required to solve this problem efficiently. The idea is to use *a-priori* information of α_t to maximize the function of unknown variables. Maximization of a function is followed by taking derivatives and equating them to zero. This will result in having no solution to some first-order conditions. The reason is due to the condition of solving for model parameters with a known distribution of unobserved data, where the distribution of the unobserved data is itself a function of model parameters. Expectation Maximization algorithm resolves such issue by iteratively approximating a distribution for the unobserved data. It estimates the model parameters by maximizing a variable that is a lower bound on the actual likelihood function of oscillation parameters, and repeats the procedure until convergence. Furthermore, to achieve convergence, numerical optimization techniques like gradient descent or Newton-Raphson could be used. However, EM algorithm comes with guarantees only of convergence to a local maximum of the defined objective function. Moreover, it gives the luxury to initialize oscillation parameters in a way that breaks symmetry in the models, thus making it a robust tool for modal parameter estimation with incomplete data. In order to integrate EM algorithm into the proposed method, a clear definition of maximum likelihood is required. This is achieved by regularizing MAP estimations for oscillations from each i -th sensor at time instant t .

C. MAP Estimations using EM-Based FB-KLPP

Consider MAP as a regularization of maximum-likelihood (ML) estimation. The relation between the unknown parameters and the observed modal measurements of oscillations will be considered by the original ML problem as¹:

$$\hat{\alpha}_t^{ML} = \arg \max_{\alpha_t} p_{\alpha_t}(\Upsilon_1, \dots, \Upsilon_T) \quad (8)$$

where $\hat{\alpha}_t^{ML}$ is the oscillation state estimate at time instant t for posterior distribution. $(\Upsilon_1, \dots, \Upsilon_T)$ denotes the measurement sequence Υ_0^T at time t , subindex α_t indicates the corresponding probability density function of $p_{\alpha_t}(\Upsilon_1, \dots, \Upsilon_T)$ parameterized by the unknown modal parameter α_t . Using conditional probability, the joint density of the oscillation observations $p_{\alpha_t}(\Upsilon_1, \dots, \Upsilon_T)$ can be written as:

$$p_{\alpha_t}(\Upsilon_1, \dots, \Upsilon_T) = p_{\alpha_t}(\Upsilon_1) \prod_{t=2}^T p_{\alpha_t}(\Upsilon_t | \Upsilon_0^{T-1}) \quad (9)$$

where $\Upsilon_0^{T-1} = (\Upsilon_0, \dots, \Upsilon_{T-1})$. Thus (8) becomes:

$$\hat{\alpha}_t^{ML} = \arg \max_{\alpha_t} p_{\alpha_t}(\Upsilon_1) \prod_{t=2}^T p_{\alpha_t}(\Upsilon_t | \Upsilon_0^{T-1}) \quad (10)$$

Also, for ideal case, the log-likelihood function can be considered as (11) rather than the regular likelihood function.

$$L_{\alpha}(\Upsilon_t) = \sum_{t=2}^T \log p_{\alpha_t}(\Upsilon_t | \Upsilon_0^{T-1}) + \log p_{\alpha_t}(\Upsilon_1) \quad (11)$$

¹ In general, *a-posteriori* probability distribution of α_t is obtained by the measurement sequence of Υ_0^T . Also, $p_{\alpha}(\Upsilon_0^T) \sim e^{-\beta J(\Upsilon_0^T)}$, where J represents a convex energy function and β is a positive parameter.

As log is a strictly increasing function, the following is equivalent to (8):

$$\hat{\alpha}_t^{ML} = \arg \max_{\alpha_t} \sum_{t=2}^T \log p_{\alpha_t}(\Upsilon_t | \Upsilon_0^{T-1}) + \log p_{\alpha_t}(\Upsilon_1) \quad (12)$$

Since observation matrix C_t for oscillation is not observable, EM algorithm is employed and instead of maximizing (12), an averaged form of the log-likelihood function is maximized.

1) *Expectation Maximization Algorithm*: The EM is derived here to acquire maximum-likelihood estimates of nearby oscillatory frequencies of each local i -th sensor/substation. This objective is achieved by computing the oscillation state estimate α_t^i from each local i -th substation given a measurement sequence $T+1$ for input C_0^T and output Υ_0^T oscillation variables. The EM algorithm [16,18] has two steps. The *E-step* is obtained with respect to the underlying unknown variables conditioned on the observations, thus maximizing the likelihood with respect to the oscillation states. The *M-step* maximizes the function as in the fully observed case to get a new oscillation state estimate of the modal parameters, thus maximizing with respect to the oscillation parameters. Note the EM model depends upon unobserved latent variables. In this formulation, the unobserved latent variable is C_t , and its realization follows a distribution with the expected value $b_t \alpha_t$. Given the current oscillation state α_t , the *E-step* finds expectation of the log-likelihood as:

$$\log L(\alpha_t | \alpha_0^{T+1}) = \mathbf{E}_{C_t | \alpha_0^T, \Upsilon_t} \log p(\alpha_t, C_t | \Upsilon_t) \quad (13)$$

where \mathbf{E} is the expected value operator. The *M-step* then chooses α_0^{T+1} to maximize the expected log-likelihood $\log(\alpha_t | \alpha_0^{T+1})$ found in the *E-step*:

$$\begin{aligned} \alpha_0^{T+1} &= \arg \max_{\alpha_t} \mathbf{E}_{C_t | \alpha_0^T, \Upsilon_t} \log p(\alpha_t, C_t | \Upsilon_t) \\ &= \arg \max_{\alpha_t} \mathbf{E}_{C_t | \alpha_0^T, \Upsilon_t} \log (p(\Upsilon_t, C_t | \alpha_t) p(\alpha_t)) \\ &= \arg \max_{\alpha_t} \mathbf{E}_{C_t | \alpha_0^T, \Upsilon_t} \sum_{C_t \in \Omega} (\Upsilon_t \log(b_t \alpha_t) - b_t \alpha_t) - \beta J(\alpha_t) \\ &= \arg \min_{\alpha_t} \sum_{C_t \in \Omega} (b_t \alpha_t - \mathbf{E}_{C_t | \alpha_0^T, \Upsilon_t} C_t \log(b_t \alpha_t)) + \beta J(\alpha_t) \end{aligned} \quad (14)$$

where Ω denotes the possible realization of α_t , $\log L = \mathbf{E}[\log L(\alpha_0^{T+1})]$. For the i -th substation, the expectation for local oscillation observation C_t^i is performed given the output Υ_t^i and the most recent voltage phase angle of oscillation estimate $\hat{\alpha}_t$. Calculating the first two moments of its individual elements $C_t^i(l)$, $l = 1, \dots, N$, the pdf is $f(C_t^i(l) | \Upsilon_t^i(l), \alpha_t^i(l))$. Applying the Bayes rule gets:

$$\begin{aligned} f(C_t^i(l) | \Upsilon_t^i(l), \alpha_t^i(l)) &= \frac{f(C_t^i(l) | \Upsilon_t^i(l), \alpha_t^i(l))}{f(\Upsilon_t^i(l) | \alpha_t^i(l))} \\ &= \frac{f(C_t^i, \Upsilon_t^i | \alpha_t)}{\sum_{C_t^i=A_1}^{A_n} f(C_t^i, \Upsilon_t^i | \alpha_t)} = \frac{f(\Upsilon_t^i | C_t^i, \alpha_t^i) f(C_t^i, \alpha_t^i)}{\sum_{C_t^i=A_1}^{A_n} f(\Upsilon_t^i | C_t^i, \alpha_t^i) f(C_t^i, \alpha_t^i)} \end{aligned} \quad (15)$$

According to normal distribution, the pdf becomes:

$$f(C_t^i(l) | \Upsilon_t^i(l), \alpha_t^i(l)) = \frac{e^{-\frac{|\Upsilon_t^i - \alpha_t^i C_t^i|^2}{\sigma_n^2}}}{\sum_{\chi=1}^n e^{-\frac{|\Upsilon_t^i - \alpha_t^i A_{\chi}|^2}{\sigma_n^2}}} \quad (16)$$

where σ_n^2 is the noise variance. The dependency on l is eliminated. It is assumed that $C_t^i(l)$ is drawn from the alphabet $A_\chi = A_1, A_2, \dots, A_n$. The calculation of moments is shown as:

First moment:

$$\mathbf{E}[C_t^i(l)|\Upsilon_t^i(l), \alpha_t^i(l)] = \frac{\sum_{\chi=1}^n A_\chi e^{\frac{-|\Upsilon_t^i(l) - \alpha_t^i(l) A_\chi|^2}{\sigma_n^2}}}{\sum_{\chi=1}^n e^{\frac{-|\Upsilon_t^i(l) - \alpha_t^i(l) A_\chi|^2}{\sigma_n^2}}} \quad (17)$$

Second moment:

$$\mathbf{E}[|C_t^i(l)|^2|\Upsilon_t^i(l), \alpha_t^i(l)] = \frac{\sum_{\chi=1}^n |A_\chi|^2 e^{\frac{-|\Upsilon_t^i(l) - \alpha_t^i(l) A_\chi|^2}{\sigma_n^2}}}{\sum_{\chi=1}^n e^{\frac{-|\Upsilon_t^i(l) - \alpha_t^i(l) A_\chi|^2}{\sigma_n^2}}} \quad (18)$$

As shown in the previous section, to achieve an optimum oscillation estimate, an initial estimation step is required.

2) *Initial Correlation Information using FB-KLPF:* Given the measurement sequence $t = 0, 1, \dots, T$ of the input and output measurements $C_t^{i^T}$ and $\Upsilon_t^{i^T}$ for an i -th sensor, the optimum oscillation estimate of $\hat{\alpha}_{t|T}^i$ can be measured by applying a FB-KLPF (See [19] for the general proof of a forward-backward Kalman filter). The novelty of KLPF is its ability to deal with the gain of the system, which is in the form of an observation function [17]. Given the MAP (or equivalently MMSE) estimate of oscillation sequence α_0^T is obtained by applying the following FB-KLPF to the state-space model (1)-(2). For the forward run, the initial condition starts from $P_{0|-1} = \text{var}(\Upsilon)$ and $\alpha_{0|-1} = 0$, showing the availability of the *a-priori* information at previous instant of time. The superscript (*) represents the transpose operator. For $t = 1, \dots, T$, calculate as shown in Eq. (19)–(24):

$$R_{e,t}^i = \sigma_n^2 I_{p+r} + C_t^i P_{t|t-1}^i C_t^{i*} \quad (19)$$

$$e_t^i = \Upsilon_t^i - C_t^i \hat{\alpha}_{t|t-1}^i \quad (20)$$

$$\hat{\alpha}_{t|t}^i = \hat{\alpha}_{t|t-1}^i + \frac{P_t^i C_t^{i*}}{C_t^i P_t^i C_t^{i*} + \sigma_\nu^2} e_t^i \quad (21)$$

$$\hat{\alpha}_{t+1|t}^i = \Phi_t \hat{\alpha}_{t|t}^i \quad (22)$$

$$\hat{P}_{t|t}^i = \hat{P}_{t|t-1}^i - \frac{P_t^i C_t^{i*}}{C_t^i P_t^i C_t^{i*} + \sigma_\nu^2} C_t^i \hat{P}_{t|t-1}^i \quad (23)$$

$$P_{t+1|t} = \Phi_t (P_{t|t-1}^i - \frac{P_t^i C_t^{i*}}{C_t^i P_t^i C_t^{i*} + \sigma_\nu^2} R_{e,t}^i) \cdot (\frac{P_t^i C_t^{i*}}{C_t^i P_t^i C_t^{i*} + \sigma_\nu^2})^* \Phi_t^* + \frac{1}{\sigma_n^2} \Gamma_t^i \Gamma_t^{i*} \quad (24)$$

For the backward run, the sequence of T observations from KLPF is required. The iteration starts from $\lambda_{T+1|T} = 0$. For $t = T, T-1, \dots, 0$, calculate as shown in Eq. (25)–(26):

$$P_{t|T}^{i^B} = F_t P_{t-1|T}^i F_t^* + \left(C_t^i P_{t|t-1}^i + \frac{P_t^i C_t^{i*}}{C_t^i P_t^i C_t^{i*} + \sigma_\nu^2} R_{e,t}^i \right) \left(\frac{P_t^i C_t^{i*}}{C_t^i P_t^i C_t^{i*} + \sigma_\nu^2} C_t^i P_{t|t-1}^i + \frac{P_t^i C_t^{i*}}{C_t^i P_t^i C_t^{i*} + \sigma_\nu^2} R_{e,t}^i \right)^T \quad (25)$$

$$\hat{\alpha}_{t|T}^i = \hat{\alpha}_{t-1|T}^i + P_{t|T}^{i^B} \quad (26)$$

where $R_{e,t}$ denotes the local oscillation covariance matrix of estimation error e_t of the i -th sensor, I_{p+r} is the identity matrix of length $p+r$, $P_{t|t-1}^i$ represents the local predicted *a-priori*

oscillation estimate covariance matrix, $\alpha_{t|t}^i$ is the local updated *a-posteriori* oscillation state estimate and $\alpha_{t|t-1}^i$ is the local predicted *a-priori* oscillation state estimate. $P_{t|t}^i$ is the local updated *a-posteriori* oscillation estimate covariance, and Q_t is the process noise correlation factor such that $Q_t = \mathbf{E}[w_t w_t^*] = \frac{1}{\sigma_n^2} \Gamma_t \Gamma_t^*$. Γ_t is the squared matrix for oscillation response. Φ_t is the state transition model applied to previous oscillation state α_{t-1} , σ_ν is the process noise variance. $P_{t|T}^{i^B}$ is the local backward-run updated *a-posteriori* oscillation estimate covariance. The desired oscillation estimate is $\hat{\alpha}_{t|T}^i$. This gives the initial oscillation estimate such that the time sequence T of oscillation measurements is known. The FB scheme of KLPF requires a considerable amount of storage and latency (latency is the measure of time delay experienced in a system). As a result, the algorithm needs to wait for all $T+1$ symbols before it can execute the backward run to obtain the state estimate. One alternate option is to reduce the time size T . Else, the filter can be ran in the forward direction only (i.e. run (19-24)) for both the initial estimation and the EM iteration with no latency.

Proof of Backward Run: This is proved in the Appendix. ■

3) *Convergence of EM Algorithm:* The following theorem proves that the negative log-likelihood of oscillations at i -th substation is decreasing over time.

Theorem II.1: Minimize the following negative log-likelihood function with α_0^T given by the following optimization problem:

$$\min_{\alpha_t \geq 0} \sum_{t=0}^T ((C_t \alpha_t + w_t) - \Upsilon_t^i \log(C_t \alpha_t + w_t)) + \beta J(\alpha_t) \quad (27)$$

where $J(\alpha_t)$ is a convex energy functional and β is a positive parameter.

The MAP estimate from each local i -th sensor is then gathered following the architecture of distributed fusion.

Proof: This is proved in the Appendix. ■

D. Distributed Filtering Fusion

The formulation of the proposed data-fusion scheme is outlined as follows. Define n -dimensional master observation oscillation variables as:

$$I_{\text{master},t} = C_{\text{master},t}^* R_{\text{master},t}^{-1} \Upsilon_{\text{master},t}, \quad I_{\text{master},t} = C_{\text{master},t}^* R_{\text{master},t}^{-1} C_{\text{master},t} \quad (28)$$

and n -dimensional local observation oscillation variables at a substation with sensor i as:

$$I_{i,t} = C_t^{i*} R_t^{i-1} \Upsilon_t^i, \quad I_i = C_t^{i*} R_t^{i-1} C_t^i \quad (29)$$

where I stands for oscillation information matrix. When the oscillation observations are distributed among the sensors installed at various substations, see Eq. (2), the master oscillation information filter can be implemented by collecting all sensor observations at a central location, or with observation fusion. This is achieved by realizing that master observation oscillation variables in (28) as [23]:

$$I_{\text{master},t} = \sum_{i=1}^N I_{i,t}, \quad I_{\text{master}} = \sum_{i=1}^N I_i \quad (30)$$

Considering the same domain and ignoring the risk of introducing additional process errors during the domain trans-

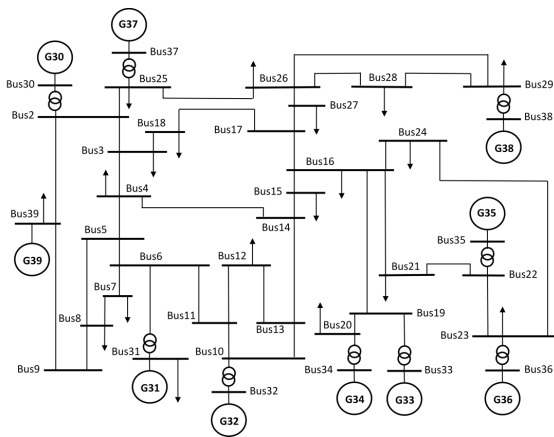


Fig. 2. Model of the IEEE 39-Bus New England System

formation, let $P_{\text{master},t|t}^{-1}$ be the updated a -posteriori oscillation estimate covariance matrix and $P_{\text{master},t|t-1}^{-1}$ be the predicted a -priori oscillation estimate covariance matrix collected from the master filter at t -th time instant. Also, $P_{\text{master},0|0}$ is the initial error covariance for the master filter. Then the master filtering measurement updates can be given by this alternate form:

$$\begin{aligned} P_{\text{master},t|t}^{-1} \hat{\alpha}_{\text{master},t|t} &= P_{\text{master},t|t-1}^{-1} \hat{\alpha}_{\text{master},t|t-1} \\ &\quad + C_{\text{master}}^* R_{\text{master}}^{-1} \Upsilon_{\text{master}} \\ P_{\text{master},t|t}^{-1} &= P_{\text{master},t|t-1}^{-1} + C_{\text{master}}^* R_{\text{master}}^{-1} C_{\text{master}} \end{aligned} \quad (31)$$

1) Convergence of the Distributed fusion:

Theorem II.2: The master error covariance matrix and the oscillation estimate are given in terms of the local covariances and estimates respectively as:

$$\begin{aligned} P_{\text{master},t|t}^{-1} &= P_{\text{master},t|t-1}^{-1} + \sum_{i=1}^N (P_{t|t-1}^{i-1} - P_{t|t}^{i-1}) \\ P_{\text{master},t|t}^{-1} \hat{\alpha}_{\text{master},t|t} &= P_{\text{master},t|t-1}^{-1} \hat{\alpha}_{\text{master},t|t-1} + \sum_{i=1}^N (P_{t|t}^{i-1} \hat{\alpha}_{t|t}^i \\ &\quad - P_{t|t-1}^{i-1} \hat{\alpha}_{t|t-1}^i) \end{aligned} \quad (32)$$

Proof: This is proved in the Appendix. ■

III. IMPLEMENTATION AND EVALUATION

The proposed method was exhaustively assessed under different network operating conditions. Among them, two of the studies are presented in this paper. Test Case I analyzed Synchrophasor measurements collected from IEEE 39-Bus New England system simulated in DIGSILENT PowerFactory ver.15 [20]. Each generator is a 6th order model and are all equipped with an Exciter (IEEET1). Apart from Gen 39, all units are installed with a Power System Stabilizer (STAB1), and a 1st order governor from [21]. Test Case II examined actual Synchrophasor measurements gathered from the New Zealand grid. In addition, the proposed method is referenced with two mainstream techniques; 1) Kalman Filter [8], and 2) Prony Analysis [22]. Damping ratios and oscillatory frequencies are computed from the master oscillation estimate $\hat{\alpha}_{\text{master},t}^i$. All detections are computed using voltage phase angles sampled at 50 Hz.

A. Test Case I: IEEE 39-Bus New England System

Referring to Fig. 2, the proposed method analyzed Synchrophasor measurements collected from Bus 15, 16, 17, 29, 30, 35, 37, 38, and 39. The predecessor, Kalman Filter, was applied to extract oscillatory information at Bus 16. By using Welch power spectral density analysis, three electromechanical oscillations were identified from measurements around Bus 16. Their pre-disturbance values are: 1) Inter-area mode with a frequency of 0.73 Hz and a damping ratio of 3.9 %, 2) Local mode with a frequency of 1.12 Hz and a damping ratio of 5.7 %, and 3) Local mode with a frequency of 1.17 Hz and a damping ratio of 5.6 %. In this study, the grid suffered from four events over a period of 60 second. They are:

- At 5 second: Bus 24 experienced a three-phase-to-ground fault, which was cleared after 0.1 second.
- At 20 second: The active power of the load connected at Bus 21 was increased by 30 % and the reactive demand by 10 %. This was ramped over 10 second.
- At 25 second: Line 16-17 experienced an outage. The line was later reconnected at 30 second.
- At 45 second: The load connected at Bus 4 increased its active and reactive power demands by 20 % and 10 %, respectively. This occurs over a 5 second ramp.

To imitate real-world dynamics, all loads were continuously perturbed with random small-magnitude fluctuations of up of 10 MW over one second. Note that the modal parameters will vary slightly due to events occurred in the system. The grid dynamics captured at Bus 16 is shown in Fig. 3(a). For this test case, the detection capability of the proposed method is compared with its Kalman Filter. The computed oscillatory parameters, over a window size of 5 seconds, are listed in TABLE I. In general, both techniques tracked the inter-area oscillation with reasonable accuracy when it is the dominating mode within the analyzed measurements. However, Kalman filter was not able to separate the two local oscillations having similar frequencies. Instead, it suffered from mode-mixing by treating the two local modes as one. The reason is Kalman Filter is originally designed to monitor the dominant mode in ringdown events [8]. Its estimation accuracy decreases when detecting electromechanical oscillations having similar frequencies or under ambient conditions. In contrast, the distributed EM-based FB KLPF was able to detect both local oscillations with reasonable precisions. This is due to its architecture of employing local filters at every metering location. The distributed architecture also provides an updated feedback for the error covariance and state estimation at each metering location.

Depending on the type of disturbance and its associated energy density, the inter-area oscillation may not be the dominant electromechanical mode in all metered locations. This can occur if the measurements are dominated by transient or ambient conditions. Consequently, the undistributed nature of Kalman Filter made it become locational dependent. For example, the local line outage event at 25 second caused the measurements collected at Bus 16 to be overwhelmed by transient dynamics. As a result, the accuracy of the estimated inter-area oscillation decreased in the 25-30 second window while the local mode remained similar to its previous estimated values. Of course, the non-linearity of transient dynamics was also contributing to the

TABLE I
TEST CASE I – NEW ENGLAND SYSTEM: DETECTING MULTIPLE OSCILLATIONS²

Measurements	ζ_{KF}	f_{KF}	ζ_D	f_D												
Time	0 s–5 s				5 s–10 s				10 s–15 s				15 s–20 s			
	3.7	0.69	3.8	0.73	4.1	0.67	4.1	0.68	4.0	0.67	4.1	0.67	4.0	0.63	4.5	0.68
	5.8	1.13	5.7	1.07	5.4	1.14	5.5	1.12	5.3	1.11	5.7	1.08	5.4	1.10	6.0	1.04
	–	–	5.6	1.17	–	–	5.6	1.16	–	–	5.8	1.10	–	–	5.6	1.16
MSE	1.3×10^{-1}		2.2×10^{-2}		2.5×10^{-1}		1.9×10^{-1}		1.4×10^{-1}		2.5×10^{-2}		1.4×10^{-1}		2.3×10^{-2}	
Time	20 s–25 s				25 s–30 s				30 s–35 s				35 s–40 s			
	4.1	0.68	4.2	0.69	3.2	0.68	4.0	0.69	3.7	0.71	3.8	0.71	3.2	0.69	3.9	0.72
	5.7	1.13	5.8	1.08	5.7	1.13	5.9	1.07	5.5	1.14	5.8	1.08	5.5	1.15	5.8	1.08
	–	–	5.9	1.11	–	–	5.6	1.14	–	–	5.7	1.13	–	–	5.6	1.14
MSE	1.3×10^{-1}		2.1×10^{-2}		4.5×10^{-1}		3.7×10^{-2}		1.4×10^{-1}		2.6×10^{-2}		3.0×10^{-2}		5.5×10^{-2}	
Time	40 s–45 s				45 s–50 s				50 s–55 s				55 s–60 s			
	3.1	0.68	3.8	0.72	3.2	0.67	3.7	0.71	3.9	0.69	3.9	0.71	3.2	0.66	3.7	0.69
	5.4	1.11	5.9	1.04	5.4	1.12	5.7	1.08	5.4	1.15	5.7	1.08	5.8	1.08	5.7	1.11
	–	–	6.1	1.05	–	–	5.5	1.15	–	–	5.4	1.15	–	–	5.7	1.15
MSE	3.0×10^{-2}		5.7×10^{-3}		3.2×10^{-2}		1.8×10^{-3}		3.2×10^{-2}		5.7×10^{-4}		3.1×10^{-2}		1.5×10^{-3}	

²In this table, ζ is the damping ratio i.e. $\zeta = \frac{-\sigma}{\sqrt{\sigma^2 + (2\pi f)^2}} \times 100$. f is the frequency in hertz, MSE is the mean-square error, subscript KF and D are the acronyms of Kalman filter and Distributed EM-Based FB KLPF scheme respectively.

estimation inaccuracies. Another example is the ambient dominated measurements collected from Bus 16 between 35 to 60 seconds. In this case, continuous load perturbations excited the local modes. In contrast, the energy of the inter-area oscillation was relatively similar to some of the load perturbations. Consequently, the estimation accuracy of inter-area mode decreased during this time. The improved accuracy in 50-55 second window may be due to the load ramp event that occurred nearby, which excited the inter-area mode.

In the contrary, the monitoring capability of the distributed EM-based FB KLPF was less impacted. By mixing with measurements obtained from healthy locations, potential estimation inaccuracies from analyzing non-linearity or ambient dominated measurements can be compensated. Even under highly ambient conditions at 55-60 second window, the proposed method demonstrated adequate noise-resistant and extracted oscillatory parameters with reasonable precisions. This can be achieved by using EM-based maximum likelihood technique to detect the incipient inter-area oscillation with the help of the observation matrix of KLPF structure.

B. Test Case II: New Zealand Network

The backbone of the New Zealand transmission infrastructure is based on 220 kV lines that are interconnected by HVDC links between North and South Islands. Being a longitudinal network with weak transmission lines, the New Zealand Grid is prone to electromechanical oscillations like those experienced by Western Systems Coordinating Council (WSCC). For this study, the proposed method was applied to track a lightly-damped inter-area oscillation occurred in the South Island between 11:12:32 am to 11:16:33 am on 30 July 2008. Synchrophasor measurements collected from Twizel (TWZ), North Makarewa (NMA), and Whakamaru (WKM) substations between 11:12:30 am to 11:13:29 am were used to further assess the detection capability of the proposed method. The system dynamics over this 60 second period is illustrated in Fig. 3(b). Whakamaru is used as the reference location for determining the phase angles. Using Welch power spectral density analysis and referring to the

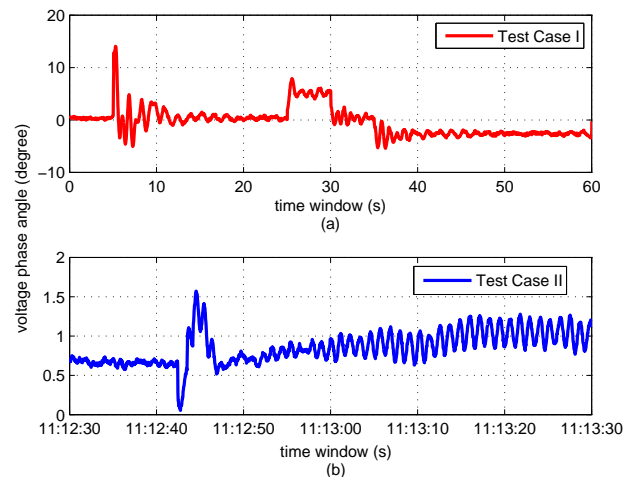


Fig. 3. a) Test Case I: Voltage Phase Angle Profile of BUS 16, b) Test Case II: Voltage Phase Angle Profile of North Makarewa (NMA) between 11:12:30 am to 11:13:29 am

report of [24], three electromechanical oscillations modes were identified. Instantaneous oscillatory parameters differ slightly from these values due to continuous changing grid operations. Their averaged values over this 60 seconds time-frame are:

- Mode 1: Inter-area oscillation with a frequency around 0.85 Hz and an averaged damping ratio of 2.0 %.
- Mode 2: Local oscillation with a frequency around 1.04 Hz with an averaged damping ratio of 5.0 %.
- Mode 3: Local oscillation with a frequency around 1.20 Hz with an averaged damping ratio of 4.9 %.

Referring to TABLE II, all three methods accurately tracked the dominant inter-area oscillation in every monitoring window. Since the two local modes have similar frequencies, Kalman Filter and Prony Analysis experienced mode-mixing problem. The two local modes were averaged and treated as one. Even so, Prony generated higher inaccuracies than Kalman Filter when detecting the damping ratio of the mixed local mode. The reason is local modes became ambient in later windows. Conse-

TABLE II
TEST CASE II – NEW ZEALAND GRID DATA: ESTIMATION RESULTS OF MULTIPLE ELECTROMECHANICAL OSCILLATIONS³

	ζ_{PR}	f_{PR}	ζ_{KF}	f_{KF}	ζ_D	f_D	ζ_{PR}	f_{PR}	ζ_{KF}	f_{KF}	ζ_D	f_D	ζ_{PR}	f_{PR}	ζ_{KF}	f_{KF}	ζ_D	f_D
Time	11:12:30 am–11:12:40 am						11:12:40 am–11:12:50 am						11:12:50 am–11:13:00 am					
	2.3	0.73	2.2	0.84	2.0	0.83	2.0	0.89	2.3	0.82	1.9	0.86	2.0	0.88	2.2	0.80	1.8	0.86
	–	–	–	–	4.9	1.02	–	–	–	–	4.9	1.01	–	–	–	–	5.0	1.01
	4.5	1.02	4.8	1.14	4.9	1.15	4.2	1.16	4.7	1.18	4.9	1.16	3.2	1.01	4.9	1.14	4.9	1.16
MSE	1.5×10^{-2}		1.5×10^{-3}		1.1×10^{-3}		1.4×10^{-2}		2.3×10^{-3}		3.6×10^{-3}		1.4×10^{-2}		2.2×10^{-3}		1.4×10^{-5}	
Time	11:13:00 am–11:13:10 am						11:13:10 am–11:13:20 am						11:13:20 am–11:13:30 am					
	2.0	0.85	1.8	0.81	2.1	0.86	2.1	0.79	2.1	0.85	2.1	0.80	1.8	0.81	2.2	0.85	2.0	0.85
	–	–	–	–	4.9	1.02	–	–	–	–	5.2	0.95	–	–	–	–	4.9	1.02
	3.2	1.20	4.9	1.17	5.0	1.18	1.8	1.12	4.8	1.18	4.9	1.18	2.4	1.05	5.3	1.12	4.9	1.15
MSE	1.4×10^{-2}		2.8×10^{-3}		5.1×10^{-5}		1.4×10^{-2}		3.6×10^{-3}		6.7×10^{-5}		1.4×10^{-2}		4.0×10^{-3}		4.1×10^{-5}	

³In this table, subscript PR is the acronym of Prony Analysis

quently, errors were incurred in modal solutions as Prony was built to track ringdown dynamics. On the other hand, the recursive nature of Kalman Filter and the proposed method allowed both techniques to better detect local oscillatory parameters under ambient-like conditions. Hence, both methods estimated the local mode with reasonable accuracies. However, the proposed method was more accurate than Kalman Filter as it did not suffer from mode-mixing issue.

IV. CONCLUSIONS

In this paper, the estimation accuracy of existing KF is enhanced using a distributed structure of EM algorithm encapsulated with initial correlation information from FB-KLPF. The proposed algorithm is able to operate under noisy/ambient conditions. It was also demonstrated to be capable of detecting oscillations having similar frequencies. Monitoring comparison of the scheme was made with existing Kalman filter and Prony analysis, which are used by the power utilities. The limitation of proposed method is the computational complexity. However, this may be resolved by assigning independent functions for each substation using parallel computing. In the future, studies to quantitatively verify the effectiveness and robustness of the proposed method to false measurements will be conducted.

APPENDIX

A. Proof of theorem II.1

For all sequences, the following constraint is satisfied:

$$\sum_{t=0}^T C_0^T + w_t^i = \Upsilon_t \quad (33)$$

To prove the convergence of EM algorithm, Υ_t is considered to be a set of perturbed data, a convex constraint optimization problem is considered using Karush-Kuhn-Tucker (KKT) conditions which have equality and inequality constraints respectively. J is a convex energy function. Assuming to satisfy (2) with Jensen's inequality, the following inequality shows:

$$\begin{aligned} & \Upsilon_t^i \log(C_t^i \alpha_0^{T+1} + w_t^i) - \Upsilon_t^i \log(C_t \alpha_0^T + w_t^i) \\ &= \Upsilon_t^i \log\left(\frac{C_t \alpha_0^{T+1} + w_t^i}{C_t \alpha_0^T + w_t^i}\right) = \Upsilon_t^i \log\left(\frac{\sum_{t=0}^T b_t \alpha_0^{T+1} + w_t^i}{C_t \alpha_0^T + w_t^i}\right) \\ &= \Upsilon_t^i \log\left(\sum_{t=0}^T \frac{b_t \alpha_0^T \alpha_0^{T+1}}{(C_t \alpha_0^T + w_t^i) \alpha_0^T} + \frac{w_t^i}{(C_t \alpha_0^T + w_t^i)}\right) \end{aligned}$$

$$\begin{aligned} &= \Upsilon_t^i \log\left(\sum_{t=0}^T \frac{C_{t+1} b_t \alpha_0^T}{\Upsilon_t^i b_t \alpha_0^T} + \frac{w_t^i}{\Upsilon_t^i}\right) \geq \Upsilon_t^i \sum_{t=0}^T \frac{C_{t+1}}{\Upsilon_t^i} \log\left(\frac{b_t \hat{\alpha}_{t+1}}{b_t \alpha_0^T}\right) \\ &= \sum_{t=0}^T C_{t+1}^i \log(b_t \alpha_0^{T+1}) - \sum_{t=0}^T C_{t+1}^i \log(b_t \alpha_0^T) \quad (34) \end{aligned}$$

In general, Jensen's inequality relates the value of a convex function of an integral to the integral of the convex function. In the context of probability theory, it is generally stated in the following form: if X is a random variable and is a convex function, then $\varphi(\mathbf{E}[X]) \leq \mathbf{E}[\varphi(X)]$. Thus inequality in (34) gives:

$$\begin{aligned} \mathbf{E}(\alpha_0^{T+1}) - \mathbf{E}(\alpha_0^T) &= \sum_{t=0}^T (C_t^i \alpha_0^{T+1} + w_t^i) - \Upsilon_t^i \log(C_t \alpha_0^{T+1} + w_t^i) \\ &+ \beta J(\alpha_0^{T+1}) - \sum_{t=0}^T (C_t^i \alpha_0^T + w_t^i) - \Upsilon_t^i \log(C_t \alpha_0^T + w_t^i) - \beta J(\alpha_0^T) \\ &\leq \sum_{t=0}^T (b_t \alpha_0^{T+1} - C_{t+1}^i \log(b_t \alpha_0^{T+1})) + \beta J(\alpha_0^{T+1}) \\ &- \sum_{t=0}^T (b_t \alpha_0^T - C_{t+1}^i \log(b_t \alpha_0^T)) - \beta J(\alpha_0^T) \leq 0. \quad (35) \end{aligned}$$

When $\mathbf{E}(\alpha_0^{T+1}) = \mathbf{E}(\alpha_0^T)$, (14) and (34) have to be satisfied. The first equality is satisfied if and only if sequence $\alpha_0^{T+1} = \alpha_0^T$ for all t , while the second one is satisfied if and only if sequence α_0^T and α_0^{T+1} are minimizers of the M -step. The functional to be minimized in M -step is strictly convex, which gives:

$$\beta \alpha_0^T \partial J(\alpha_0^T) + \sum_{t=0}^T b_t \alpha_0^T - \sum_{t=0}^T \Upsilon_{t+1}^i = 0 \quad (36)$$

After plugging the moments into these equations, it gives:

$$\beta \alpha_0^T \partial J(\alpha_0^T) + \sum_{t=0}^T b_t \alpha_0^T - \sum_{t=0}^T e^{\frac{-1|\Upsilon_t^i - \alpha_0^T C_t^i|^2}{\sigma_n^2}} \quad (37)$$

Therefore, oscillation state sequence α_0^T is one minimizer of the original problem.

B. Proof of theorem II.2

The master oscillation estimate is given by

$$\begin{aligned} P_{\text{master},t|t}^{-1} \hat{\alpha}_{\text{master},t|t} &= P_{\text{master},t|t-1}^{-1} \hat{\alpha}_{\text{master},t|t-1} + C_{\text{master}}^* R_{\text{master}}^{-1} \Upsilon_{\text{master},t} \\ P_{\text{master},t|t}^{-1} &= P_{\text{master},t|t-1}^{-1} + C_{\text{master}}^* R_{\text{master}}^{-1} C_{\text{master}} \quad (38) \end{aligned}$$

Since R_{master} is block diagonal, the terms $C_{\text{master}}^* R_{\text{master}}^{-1} \Upsilon_{\text{master},t}$ and $C_{\text{master}}^* R_{\text{master}}^{-1} C_{\text{master}}$ are decomposed into the sums

$$C_{\text{master}}^* R_{\text{master}}^{-1} \Upsilon_{\text{master},t} = \sum_{i=1}^N H^{i*} R^{i-1} \Upsilon_t^i$$

$$C_{\text{master}}^* R_{\text{master}}^{-1} C_{\text{master}} = \sum_{i=1}^N C^{i*} R^{i-1} C^i \quad (39)$$

Noting for the i -th sensor, the oscillation estimate and the error covariance are given by

$$P_{t|t}^{i-1} \hat{\alpha}_{t|t}^i = P_{t|t-1}^{i-1} \hat{\alpha}_{t|t-1}^i + C^{i*} R^{i-1} \Upsilon_t^i$$

$$P_{\text{master},t|t}^{-1} = P_{\text{master},t|t-1}^{-1} + C^{i*} R^{i-1} C^i \quad (40)$$

which shows that the master filter is upgraded after sending the feedback about oscillations and getting updated results from i -th number of sensors.

C. Proof of Backward-run of KLPF

For calculating the local backward-run updated a – *posteriori* oscillation estimate covariance $P_{t|T}^{iB}$, take the difference between (21) and (1). Let $\frac{P_t^i C_t^{i*}}{C_t^i P_t^i C_t^{i*} + \sigma_v^2}$ from (21) is equal to Λ_t , and inserting the value of Υ_t^i from (2).

$$\alpha_{t+1}^i - \hat{\alpha}_{t|t}^i = F_t P_{t-1|t-1}^i F_t^* + \mathbf{E}[(\Lambda_t (\Upsilon_t^i - C_t \alpha_{t|t-1}^i) - v_t) (\Lambda_t (\Upsilon_t^i - C_t \alpha_{t|t-1}^i) - v_t)^*]$$

$$P_{t|T}^{iB} = F_t P_{t-1|t-1}^i F_t^* + [(\Lambda_t C_t P_{t|t-1}^i + \Lambda_t R_{e,t}^i) (\Lambda_t C_t P_{t|t-1}^i + \Lambda_t R_{e,t}^i)^*]$$

$$P_{t|T}^{iB} = F_t P_{t-1|t-1}^i F_t^T [(\Lambda_t C_t P_{t|t-1}^i + \Lambda_t R_{e,t}^i) (\Lambda_t C_t P_{t|t-1}^i + \Lambda_t R_{e,t}^i)^*] \quad (41)$$

The value of local backward-run updated a – *posteriori* oscillation estimate covariance $P_{t|T}^{iB}$ will then be added to the updated oscillation state estimate $\alpha_{t|T}^i$ to give (26).

ACKNOWLEDGMENT

The authors would like to thank Transpower New Zealand for providing Synchrophasor measurements, and Professor James L. Kirtley from Massachusetts Institute of Technology (MIT) for his insights and suggestions during the development of the work presented in this paper.

REFERENCES

- [1] Rogers, G., ‘Power system oscillations’, *Norwell, MA: Kluwer*, 2000.
- [2] Peng, J. C.-H. and Nair, N. K. C., ‘Enhancing Kalman filter for tracking ringdown electromechanical oscillations’, in *IEEE Transactions on Power Systems*, vol. 27(2), pp. 1042–1050, May 2012.
- [3] Phadke, A. and Thorp, J., ‘Synchronized phasor measurements and their applications’, *New York: Springer*, 2008.
- [4] Kundur, P., ‘Power system stability and control’, London, U.K.: McGraw-Hill, 1994.
- [5] Sanchez-Gasca, J. J. and Chow, J., ‘Performance comparison of three identification methods for the analysis of electromechanical oscillations’, *IEEE Trans. Power Syst.*, vol. 14(3), pp. 995–1002, August 1999.
- [6] Sarmadi, S. A. and Venkatasubramanian, V., ‘Electromechanical mode estimation using recursive adaptive stochastic subspace identification’, *IEEE Trans. Power Syst.*, vol. 29(1), pp. 349–358, January 2014.
- [7] Zhou, N., ‘Electromechanical mode online estimation using regularized robust RLS methods’, *IEEE Trans. Power Syst.*, vol. 23(4), pp. 1670–1680, November 2008.

- [8] Korba, P., ‘Real-time monitoring of electromechanical oscillations in power systems: First findings’, *IET Gen., Transm., Distrib.*, vol. 1, pp. 80–88, 2007.
- [9] Yang, J. -Z., ‘A hybrid method for the estimation of power system low-frequency oscillation parameters’, *IEEE Trans. Power Syst.*, vol. 22(4), pp. 2115–2123, November 2007.
- [10] Kamwa, I., ‘Robust detection and analysis of power system oscillations using the Teager-Kaiser energy operator’, *IEEE Trans. Power Syst.*, vol. 26(1), pp. 323–333, February 2011.
- [11] Messina, A. R., ‘Interpretation and visualization of wide-area PMU measurements using Hilbert analysis’, *IEEE Trans. Power Syst.*, vol. 21(4), pp. 1763–1771, November 2006.
- [12] El-Naggar, K. M., ‘On-line measurement of low-frequency oscillations in power systems’, *Elsevier Meas. J.*, vol. 42, pp. 716–721, 2009.
- [13] Wiltshire, R. A., ‘A Kalman filtering approach to rapidly detecting modal changes in power systems’, *IEEE Trans. Power Syst.*, vol. 22(4), pp. 1698–1706, November 2007.
- [14] Hauer, J. F., Demeure, C. J., and Scharf, L. L., ‘Initial results in Prony analysis of power system response signals’, *IEEE Trans. Power Syst.*, vol. 5(1), pp. 80–89, February 1990.
- [15] Messina, et al., A. R., ‘Inter-area oscillations in power systems: A nonlinear and nonstationary perspective’, *Springer*, 2009.
- [16] Mahmoud, M. S., and Khalid, H. M., ‘Expectation maximization approach to data-based fault diagnostics’, *Elsevier- Information Sciences, Special section on ‘Data-based Control, Decision, Scheduling and Fault Diagnostics’*, vol. 235, pp. 80–96, June 2013.
- [17] Sukhavasi, R. T., Hassibi, B., ‘The Kalman like particle filter: Optimal estimation with quantized innovations/measurements’, *IEEE Annual Conference on Decision and Control (CDC)*, 2009, pp. 4446–4451.
- [18] Naffouri, T. Y., ‘An EM-based forward-backward Kalman filter for the estimation of time-variant channels in OFDM’, *IEEE Transactions on Signal Processing*, vol. 1(11), pp. 1–7, November 2006.
- [19] Kailath, T., Syed, A. H., and Hassibi, B., ‘Linear estimation’, *Prentice Hall*, 2000.
- [20] DiGSILENT, ‘DiGSILENT technical documentation ver. 15’, *DiGSILENT GmbH*, 2013.
- [21] Zhang, Y., ‘Design of wide-area damping control systems for power system low-frequency inter-area oscillations’, *PhD thesis*, Washington State University, Seattle, USA, 2007.
- [22] Hauer, J. F., ‘Application of Prony analysis to the determination of modal content and equivalent models for measured power system response’, *IEEE Trans. Power Syst.*, vol.6(3), pp. 1062–1068, August 1991.
- [23] Saber, R. O., ‘Distributed Kalman filters with embedded consensus filters’, in *Proc. 44th IEEE Conf. Decision Control*, Seville, Spain, pp. 8179–8184, December 2005.
- [24] Hay, K. and Wilson, D., ‘Psynmetrix monthly report for transpower NZ’, *Psynmetrix*, 2008.



Haris M. Khalid (M’13) received his M.S and Ph.D. degrees from King Fahd University of Petroleum and Minerals (KFUPM), Dhahran, Kingdom of Saudi Arabia, in 2009 and 2012, respectively. He has worked as a research fellow at Distributed Control Research Group at KFUPM. Since 2013, he has been working as a Postdoctoral Researcher with Department of Electrical Engineering and Computer Science at Masdar Institute of Science and Technology (MI) collaborated with MI-MIT Cooperative Program. His research interests are power systems, signal processing, fault diagnostics, filtering, estimation, performance monitoring and battery management systems.



Jimmy C. -H. Peng (S’05-M’12) received the B.E. (Hons.) and Ph.D. degrees from the University of Auckland, Auckland, New Zealand, in 2008 and 2012, respectively. In 2012, he joined the Department of Electrical Engineering and Computer Science at Masdar Institute of Science and Technology, Abu Dhabi, United Arab Emirates, as an Assistant Professor of Electrical Power Engineering. He was a Visiting Scientist with the Research Laboratory of Electronics (RLE) and a Visiting Assistant Professor with the MIT-MI Cooperative Program at Massachusetts Institute of Technology (MIT), in 2013 and 2014, respectively. His research interests are power system stability, synchrophasor measurements, real-time system identification, and high performance computing.